On Irregular, Nonlinear Waves in a Spread Sea

P. Jonathan

P. H. Taylor[1]

Shell Research B.V.,
P.O. Box 60,
2280 AB Rijswijk ZH, The Netherlands

Optimal design and reassessment of offshore structures requires a good understanding of the ocean environment. The motion of the sea surface can be viewed as a three-dimensional, nonlinear stochastic process in time. In order to characterize the wave environment adequately, we need to model its random, nonlinear, and spread nature. In this paper, we address:

- *the expected shape of a wave near a crest or trough,*
- *the expected shape of the ocean surface at one point, given a crest at a different point,*
- *an efficient method to incorporate nonlinear effects within linear wave simulations,*
- *the magnitude of wave nonlinearity as a function of wave amplitude.*

Detailed comparison of theory and full-scale offshore measurements at the Shell Expro Tern platform show good agreement.

1 Introduction

Safe and cost-effective production of oil and gas from offshore platforms requires robust methods to assess the reliability of the offshore structure. This assessment, in turn, requires a good understanding of the ocean environment at the location of the structure.

In this paper, we examine ocean surface time-series recorded at the Shell Expro Tern platform. The objective of the analysis is to validate some of the existing theory for the behavior and properties of the ocean surface, required for design and assessment purposes. Since the sea surface can be modeled as a three-dimensional, nonlinear random process, we consider different aspects of the sea's random, nonlinear, and spread nature in the following sections.

The Tern platform is located in the northern North Sea, between the Shetland Isles and Norway, about 100 mi offshore, in about 170 m of water. The structure consists of a piled steel jacket and topsides, together weighing about 21,000 tonnes. Tern is equipped with a monitoring system comprised of strain gages positioned near the base of the four corner legs, a wind sensor placed on top of the derrick, two wave-height sensors at different locations, and a water-particle velocity meter attached to the jacket at −41 m. The wave height sensors are, respectively, an EMI laser sensor and a MAREX radar sensor, and the particle velocity meter is a Marsh-McBirney electromagnetic type. A schematic diagram of the Tern platform and environmental sensors is given in Fig. 1.

Since its installation in 1988, Tern has experienced a number of severe winter storms. In this paper, we use time-histories of surface elevation recorded during 9 h of the winter storm of January 3/4, 1993 to validate the various theoretical models presented. For the 9 h of data used, the storm conditions were effectively uniform. The hourly H_S was approximately constant at about 12 m, with an hourly peak period T_P of approximately 14 s. The mean hourly surface spectrum estimated from EMI sensor measurements at Tern is shown in Fig. 2. Surface spectra for each hour of the storm were found to exhibit a ω^{-4} spectral tail (see, for example, Donelan et al., 1985; and Phillips, 1985). The mean wave direction, measured counterclockwise from platform East, was approximately 250 deg (see Fig. 1). Further details of the storm data recorded are given by Jonathan et al. (1994).

In this article we first consider the expected form of a wave in time, comparing Tern measurements with the theoretical results of Lindgren (1970) (see Section 2). Then in Section 3, using a simple model to describe the observed directional spreading effects at Tern, we estimate the expected wave profile at one point, given that a crest occurs at some different point. Realistic simulation of ocean surface time-series requires a method to incorporate the effects of wave nonlinearity; we present an approach based on the work of Creamer et al. (1989). We use this method to simulate storm data which is directly comparable to the 9 h of measurements at Tern for the storm of interest. We compare crest and trough distributions for measured and simulated data, and also estimate the magnitude of wave nonlinearity for crests and troughs of different sizes (see Section 4).

2 The Expected Shape of a Linear Wave

We first consider the expected form of a wave in a linear, unidirectional Gaussian sea model. We describe the ocean surface, in the usual way, as a linear Gaussian process of the form

$$Y_t = \sum_{n=1}^{N} A_n \cos(\omega_n t) + B_n \sin(\omega_n t) \tag{1}$$

where A_n, B_n are independent normal random variables with zero means whose variance σ_n^2 is defined by the surface spectrum $S(\omega)$:$\sigma_n^2 = \int_{\omega_n}^{\omega_{n+1}} S(\omega) d\omega$. The form Li_t for the expected shape near an arbitrary crest was developed by Lindgren (1970), and shown to be

$$\mathrm{Li}_t = a\left(r_t - \frac{\sigma^2}{a^2}\left(r_t + \frac{\dot{r}_t}{\lambda^2}\right)\left(\frac{\sqrt{2\pi}\gamma e^{\gamma^2/2}\Phi(\gamma)}{1 + \sqrt{2\pi}\gamma e^{\gamma^2/2}\Phi(\gamma)}\right)\right) \tag{2}$$

where r_t is the autocorrelation function for the Gaussian surface in time, and γ is a measure for narrow-bandedness for a surface elevation a, given by $\gamma = \lambda^2 a/\sqrt{\sigma^2(\upsilon^4 - \lambda^4)}$. $\lambda^2\sigma^2$ and $\upsilon^4\sigma^2$ are the second and fourth spectral moments, respectively, and Φ is the cumulative distribution function for a standard normal random variable.

[1] Author for correspondence.

Contributed by the OMAE Division and presented at the 14th International Symposium and Exhibit on Offshore Mechanics and Arctic Engineering, Copenhagen, Denmark, June 18–20, 1995, of THE AMERICAN SOCIETY OF MECHANICAL ENGINEERS. Manuscript received by the OMAE Division, 1995; revised manuscript received September 25, 1996. Technical Editor: S. K. Chakrabarti.

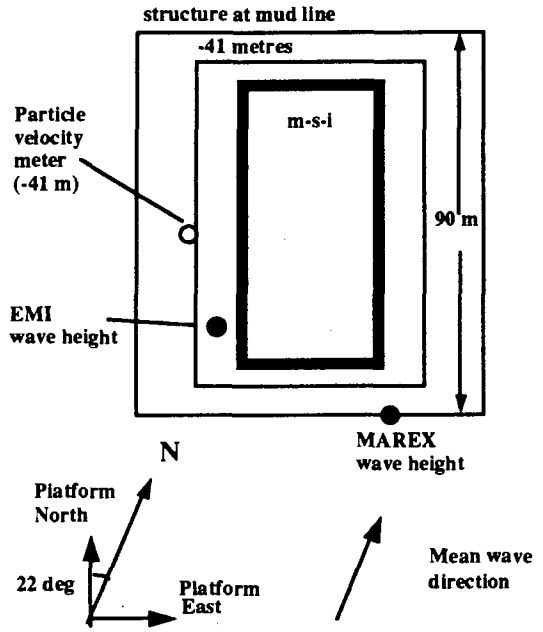

Fig. 1 Schematic of Tern structure

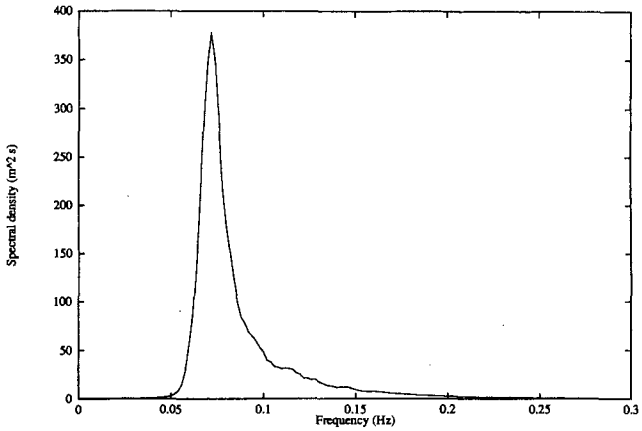

Fig. 2 Average hourly surface spectral density at EMI

Li_t is a nonlinear function of crest elevation a in general. However, as the crest elevation is increased, the Lindgren profile converges to ar_t, which is simply the autocorrelation function scaled by the crest amplitude. Tromans et al. (1991) make use of this result in their NewWave model used for the design and reassessment of drag-dominated structures.

Phillips et al. (1993, 1994) report good agreement between the average measured temporal and spatial profiles of ocean waves with the appropriate (scaled) autocorrelation functions. Theoretical predictions Li_t and ar_t based on the surface spectrum for the winter storm of 1993 at Tern, as shown in Fig. 3(a, b), for crest elevations of 2 m and 6.5 m. Also shown are 95-percent confidence intervals for the mean measured profiles near the corresponding crests at Tern. In order to facilitate the comparison of linear theory with measurements, the measured profiles were linearized to remove the effects of vertical crest-trough asymmetry, according to the approach discussed in Section 4. It can be seen, from Fig. 3(a), that the full solution Li_t is superior to ar_t for small and intermediate-sized crests. For large crests (Fig. 3(b)), the scaled autocorrelation ar_t also gives excellent agreement with measurements.

3 Directional Spreading: Expected Wave Shape at a Distant Point

The ocean surface is three-dimensional. In order to incorporate the effects of a spread sea within uni-directional wave loading studies, a directional spreading in-line velocity reduction factor is applied. Accurate estimation of this spreading factor is therefore important for computational studies of structural reliability. Jonathan et al. (1994) estimated directional spreading factors for the winter storm of January 3/4, 1993 at Tern using particle velocity measurements, and showed that a velocity reduction factor of 0.9 was appropriate.

It is important to check that estimates for directional spreading factors, and models for directional spreading, give a reasonable physical insight to the ocean environment at Tern. We can do this by predicting some property of the spread sea at Tern using theory alone, and then validating the prediction using independent field data. For example, using the theory outlined in the foregoing, together with a sensible model for directional spreading, it is possible to predict the expected shape of the ocean surface at one point, given that a crest (or trough) occurs at a different point. The prediction can then be validated against measurement. Using the reverse argument, it should be possible to estimate directional spreading given time-series from two different surface elevation sensors.

For the 1993 winter storm, we have measured the average time-series recorded at the MAREX sensor given that a crest with linear component a occurs at the EMI sensor, and vice versa (see Fig. 1). We have also examined the conditional profile at one sensor given a trough at the other sensor. A typical result (representative of a comprehensive set of comparisons available from the authors) is given in Fig. 4, for conditioning on a crest of 10–12 m. The figure gives 95-percent confidence intervals for the mean conditional profiles, and indicates excellent agreement between the respective sets of profiles. Further, extending Lindgren's theory, it can be shown that

Nomenclature

x, y = coordinates
θ = angle
ω = angular frequency
k = wave number
Φ = cumulant for standard normal distribution
A, B = normally distributed random variables
Y = Gaussian process for ocean surface
S = surface spectrum
σ^2 = surface variance
$\lambda^2\sigma^2$ = second moment of S
$\upsilon^4\sigma^2$ = fourth moment of S
γ = broad-bandedness
H_S = hourly significant wave height
T_P = hourly peak period
r = autocorrelation function of surface
Li = Lindgren profile
H = directional spreading function
σ_θ^2 = variance of directional spreading function
a = linear surface extremum
c = measured ocean crest
t = measured ocean trough
β = second-order nonlinearity of surface
η = realization of ocean surface
$\tilde{\eta}$ = Hilbert transform of η
$\overline{\eta}$ = spatial Fourier transform of η

Subscript

t = time

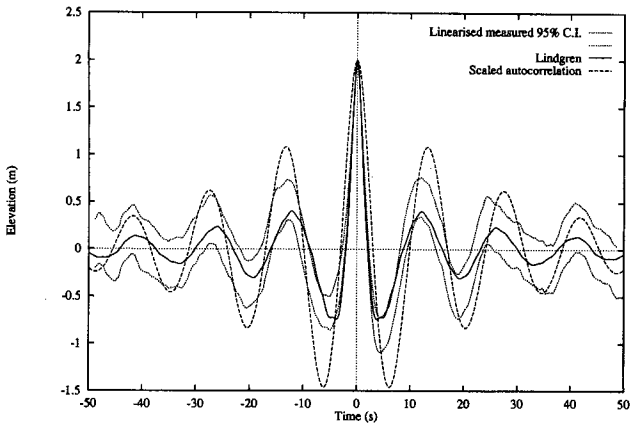

Fig. 3(*a*) Expected profile at EMI for crests of 2.0 m

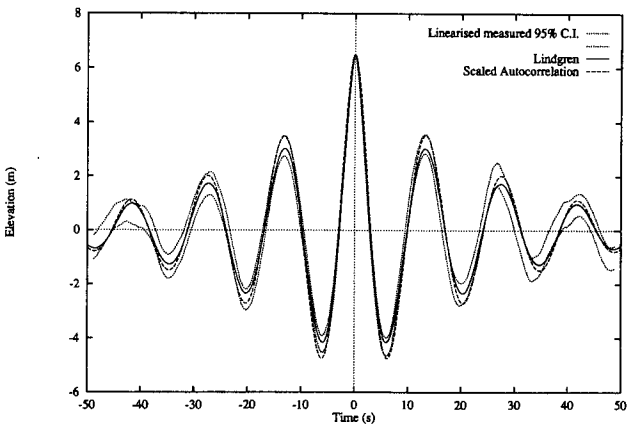

Fig. 3(*b*) Expected profile for crests of 6.5 m

$$(Y_{\text{sensor1},t} \mid Y_{\text{sensor2},0} = a,\ \dot{Y}_{\text{sensor2},0} = 0)$$

$$= a \int\int_{0-\pi}^{\infty\pi} \left(1 - \frac{\sigma^2}{a^2}\left(1 - \frac{\omega^2}{\lambda^2}\right)\right)\left(\frac{\sqrt{2\pi}\gamma e^{\gamma^2/2}\Phi(\gamma)}{1 + \sqrt{2\pi}\gamma e^{\gamma^2/2}\Phi(\gamma)}\right)$$

$$\times H(\omega, \theta; \theta_0, \sigma_\theta) \cos(kx \cos\theta + ky \sin\theta - \omega t) d\theta d\omega \quad (3)$$

for the appropriate displacements x and y, and spreading function $H(\theta_0, \sigma_\theta; \omega, \theta)$ for mean wave direction θ_0 and spreading parameter σ_θ estimated from the Tern data. We chose to use a wrapped-normal spreading function

$$H(\omega, \theta; \theta_0, \sigma_\theta) = \frac{1}{\sqrt{2\pi\sigma_\theta^2(\omega)}} \exp\left(-\frac{(\theta - \theta_0(\omega))^2}{2\sigma_\theta^2(\omega)}\right) \quad (4)$$

for this analysis. Using Eqs. (3) and (4), the time-series at one sensor corresponding to crests (of different sizes) at the other were estimated, using a frequency-independent value for σ_θ of 30 deg (consistent with an effective velocity reduction factor of approximately 0.9 determined independently). The result is also shown in Fig. 4. The agreement between measurement and theory is excellent.

In a long-crested sea, we would expect that the average crest elevation at the respective sensor locations would be equal, but that the times at which crests occur at the sensor locations would be different in general. Figure 4 clearly demonstrates that the measured large waves are short-crested, because the crest elevations at the respective sensors are significantly different on average; we have a 10–12-m crest at the conditioning sensor, but a ~8-m crest at the second sensor. Despite the different nature of the EMI and MAREX sensors, the fact that the results for MAREX|EMI and EMI|MAREX agree well shows that these instruments provide consistent descriptions of the average conditional temporal structure of ocean waves. In particular, for data analyzed here, there is no evidence to suggest that the effects of sea spray, foam, or structural interference influence one sensor more than the other on average. Note that there is almost no time-shift between the MAREX and EMI crests. This is due to the fact that the mean wave direction for the storm in question is almost perpendicular to the straight line through the EMI and MAREX sensor locations (Fig. 1).

The distance between the MAREX and EMI sensors is in the region of 40 m; this is comparable to the size of typical offshore structures. The present analysis clearly demonstrates that accurate knowledge of the spatial coherence of large waves over this length scale is crucial for reliable prediction of wave-structure interaction (see Battjes, 1982; and Jonathan and Taylor, 1996).

4 Wave Nonlinearity

Real ocean waves exhibit nonlinearity. Nonlinearity is introduced into standard models for the ocean surface by the boundary conditions at the free-surface. For small crests (or troughs), the effects of wave nonlinearity are relatively small. However, as the size of the surface displacement from mean sea level increases, then the influence of wave nonlinearity increases.

The size of the lowest-order nonlinear effect is equal for both crests and troughs. That is, given a linear crest component of magnitude a and a linear trough component of magnitude $-a$, then the corresponding full crest c and trough t (correct to second order) are $c = a + \beta$ and $t = -a + \beta$ where β is the nonlinear component. For a Stokes wave, it is well known that $\beta = 0.5\ ka^2$ to second order for waves on deep water. For the real sea, with broad-banded spectrum, the expression of β depends on both spectral form and wave amplitude.

Once we have estimated the form of β for a given sea state, we can use the foregoing theory to obtain estimates of linearized ocean surface time-series direct from offshore measurements. Suppose that we are interested in estimating the expected linearized profile of a wave near a crest with linear component a. Knowing β, we can extract the local profiles of all crests $c \cong a + \beta$ and troughs $t \cong -a + \beta$ recorded offshore. We can then subtract the averaged crest and trough profiles obtained in order to remove nonlinear components, at least to leading order: $a = (c - t)/2$. This is the method used to linearize measured time-series in this paper.

Realistic simulation of the ocean surface requires faithful incorporation of nonlinear effects. This can be achieved by Stokes-type perturbation solutions of the water-wave problem. However, Creamer et al. (1989) have devised a more efficient method to incorporate nonlinear components within linear wave simulations. They expand the Hamiltonian for the water wave

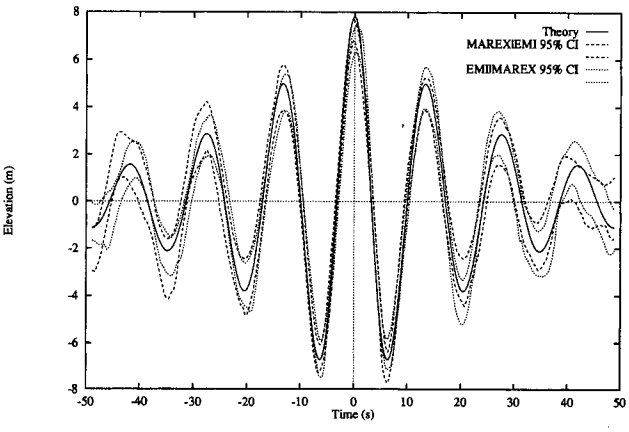

Fig. 4 Conditional linearized profiles: (condition = crest 10.0–12.0 m)

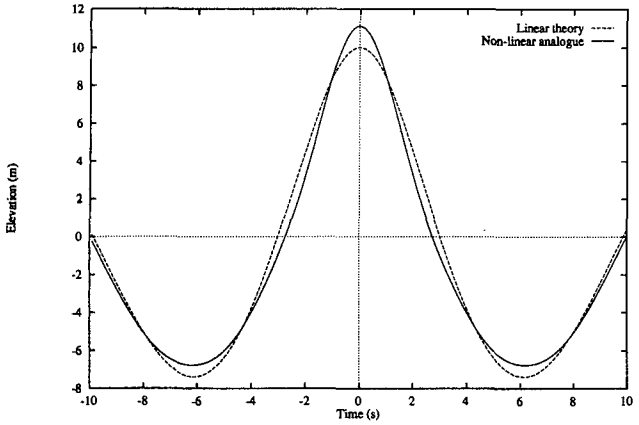

Fig. 5 Effect of nonlinearity on expected wave profile

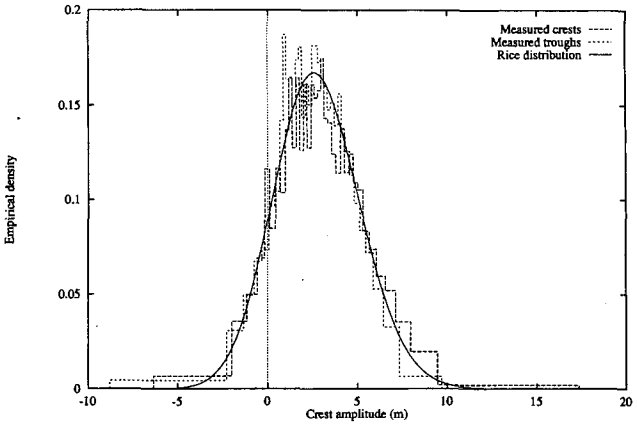

Fig. 6 Crest and trough distributions at Tern

problem in terms of the potential at the free surface ϕ_S and the free surface η itself. They then seek a transformation of canonical variables ϕ_S and η which eliminates the second-order term in the Hamiltonian expansion. This transformation eliminates the lowest-order nonlinearity in the problem; the same transformation can thus be used to turn linear representations of the ocean surface to nonlinear time-series, correct to second order in nonlinearity. In practical terms, Creamer's method can be expressed just in terms of a sequence of Fourier transforms (see Taylor, 1992), which can be executed numerically with high efficiency. The kth Fourier component $\overline{\eta}_k$ of the transformed free surface is given by

$$\overline{\eta}_k = \frac{1}{|k|}\int_{-\infty}^{\infty} dy e^{-iky}(e^{ik\tilde{\eta}(y)} - 1) \qquad (5)$$

where $\tilde{\eta}$ is the Hilbert transform of the linear free surface.

The Creamer method can be used to explore the effects of nonlinearity on the expected profile in time. Figure 5 shows the corresponding linear and nonlinear profiles for a large crest condition. The crest of the nonlinear profile is higher than its linear counterpart. Similarly, the local troughs at +/− 6s are shallower for the nonlinear profile. Note also that the nonlinear crest is sharper, and the nonlinear troughs more rounded.

5 Comparison of Offshore Measurements and Nonlinear Simulation

The main application of the Creamer method outlined in the foregoing is the realistic simulation of ocean surface time-series. Using the approach, we have simulated 9 h of time-series data for the ocean surface, using the average spectral form for the 1993 winter storm at Tern. The objective of the analysis is to determine whether our computational model is consistent with offshore measurements, by comparing the statistics of simulated time-series with those of the 9 h of recorded data.

First, 9 h of time-series were generated using the linear wave model described in Section 2. The Creamer method was then used to incorporate nonlinear components within these time-series. The skewness of the original "linear" time-series was found to be 0.0, whereas the transformed "nonlinear" series exhibited a skewness of +0.2, indicating crest-trough asymmetry; crests are larger than troughs in general. Figure 6 shows crest and trough distributions for the measured Tern data, together with the theoretical Rice distribution. The largest crests are bigger than the largest troughs. In addition, the skewness of the measured time-series was found to be +0.2. We conclude that the Tern measurements also exhibit crest-trough asymmetry, as expected.

Estimating Nonlinearity for Crests and Troughs. The results of the simulations can be used to estimate the value of the crest and trough component β due to nonlinearity, in a number of ways. Perhaps the simplest method is to detect all crests in some size range found in the "linear" time-series. Then identify all the corresponding crests in the "nonlinear" time-series. The average difference between the "nonlinear" and "linear" crests is therefore an estimate for β, for crests in that size range. Alternatively, we have devised an approach for constrained simulation of ocean waves (Taylor et al., 1995) which enables crests of particular sizes to be embedded within an otherwise arbitrary time-history, so that the statistical properties of the modified time-histories are statistically almost indistinguishable from those of random time-histories which just happen to contain a crest of the desired size. The method is similar to that proposed by Borgman (1990), and provides a very efficient approach to generating time-series guaranteed to contain the crest of interest. The values of β, estimated by this means, are equal to those obtained from the 9 h of simulated data, to within statistical variability. Figure 7 shows a plot of the average nonlinear component to crests, as a function of linear crest component in the range 2 m−12 m, in terms of 95-percent confidence intervals for the value of β.

Unfortunately, we cannot estimate the nonlinear component β for the measured data at Tern using this approach, since we do not have access to the corresponding "linear" ocean surface! However, we can estimate β by sorting the crests c and troughs t measured at Tern. If we then pair off the crests and troughs (from the largest to the smallest), we can estimate the magnitude of the corresponding linearized extreme using $a = (c -$

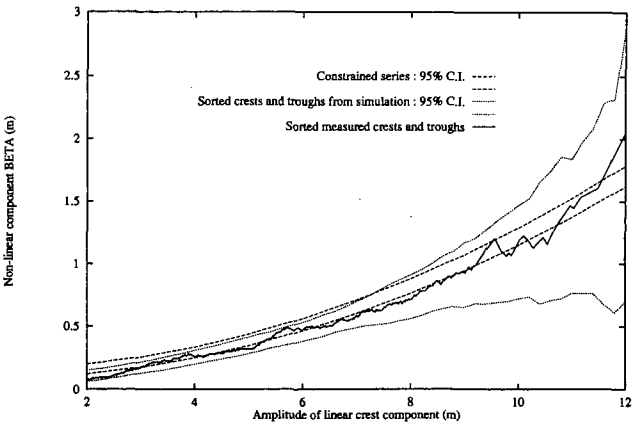

Fig. 7 Estimation of wave nonlinearity

$t)/2$ and estimate the nonlinearity as $\beta = (c + t)/2$. The result of performing this calculation for the measured Tern data is also shown in Fig. 7. We have performed the same sorting operation for 100 different realizations of the 9 h of simulated nonlinear data; results are shown in Fig. 7, again in terms of 95-percent confidence intervals for the value of β. It can be seen that there is good agreement between the three sets of curves for the whole range; in particular, the agreement between the two sets of curves based on sorted crests and troughs is excellent. Note, however, that confidence intervals for β estimated using the sorted crest and trough simulations diverge with increasing crests amplitude, due to sparsity of data.

The fact that the curve based on measured data is not significantly different to the results based on second-order simulations, suggests that measured crest-trough asymmetry at Tern can be adequately modeled using second-order wave theory. This conclusion has important engineering implications; for example, in the estimation of *air-gap* for offshore structures. Further analysis is under way.

6 Conclusions

In this work, we have outlined existing theory for the expected profile of a wave near a crest or trough, and demonstrated good agreement between theory and measurements at Tern. For large crests, after accounting for surface nonlinearity, the expected profile converges to the (appropriately scaled) autocorrelation function for the underlying wave field.

Using a simple wrapped-normal spreading function, and the directional spreading factor estimated from the Tern data, we can predict the average wave shape at a distant point. This result gives confidence that our physical understanding of the spread sea at Tern can be used reliably to make predictions about the wave environment there.

The method of Creamer et al. (1989) provides an efficient method to simulate time-series of the ocean surface realistically, correct to second-order in nonlinearity. Simulation results are in good agreement with offshore measurements at least for crests up to 12 m.

Acknowledgment

The authors wish to thank George Z. Forristall for enlightening discussions, and the reviewer for a number of helpful comments.

References

Battjes, J. A., 1982, "Effects of Short-Crestedness on Wave Loads on Long Structures," *Applied Ocean Research,* Vol. 4, pp. 165–172.

Borgman, L. E., 1990, "Irregular Ocean Waves: Kinematics and Forces," *The Sea,* Vol. 9A, eds., B. Le Méhauté and D. M. Hanes, Wiley-Interscience, New York, NY, pp. 121–168.

Creamer, D. B., Henyey F., Schult, R., and Wright, J., 1989, "Improved Linear Representation of Ocean Surface Waves," *Journal of Fluid Mechanics,* Vol. 205, pp. 135–161.

Dean, R. G., and Sharma, J. N., 1981, "Simulation of Wave Systems due to Non-Linear Directional Spectra," *Proceedings, International Symposium on Hydrodynamics in Ocean Engineering,* Vol. 2, Norwegian Institute of Technology, Trondheim, Norway, pp. 1211–1222.

Donelan, M. A., Hamilton, J., and Hui, W. H., 1985, "Directional Spectra of Wind-Generated Waves," *Philosophical Transactions Royal Society London,* Vol. A315, pp. 509–562.

Jonathan, P., Taylor, P. H., and Tromans, P. S., 1994, "Storm Waves in the Northern North Sea," *Proceedings, 7th International Conference on the Behaviour of Offshore Structures,* ed., C. Chryssostomidis, Vol. 2, Pergamon, Oxford, U.K., pp. 481–494.

Jonathan, P., and Taylor, P. H., 1996, "Wave-Induced Loads on Fixed Offshore Structures," presented at OMAE'96, Florence, Italy.

Lindgren, G., 1970, "Some Properties of a Normal Process Near a Local Maximum," *Annals of Mathematical Statistics,* Vol. 41, pp. 1870–1883.

Phillips, O. M., 1985, "Spectral and Statistical Properties of the Equilibrium Range in Wind-Generated Gravity Waves," *Journal of Fluid Mechanics,* Vol. 156, pp. 505–531.

Phillips, O. M., Gu, D., and Donelan, M., 1993a, "Expected Structure of Extreme Waves in a Gaussian Sea. Part I: Theory and SWADE Buoy Measurements," *Journal of Physics of Oceanography,* Vol. 23, pp. 992–1000.

Phillips, O. M., Gu, D., and Walsh, E. J., 1993b, "Expected Structure of Extreme Waves in a Gaussian Sea. Part 2: SWADE Scanning Radar Altimeter Measurements," *Journal of Physics of Oceanography,* Vol. 23, pp. 2297–2309.

Phillips, O. M., 1994, "The Structure of Extreme Waves," *Proceedings, 20th Symposium on Naval Hydrodynamics,* Santa Barbara, CA.

Taylor, P. H., 1992, "On the Kinematics of Large Ocean Waves," *Proceedings, 6th International Conference of the Behaviour of Offshore Structures* (BOSS '92), Vol. 1, pp. 134–145.

Taylor, P. H., Jonathan, P., and Harland, L., 1995, "Time-Domain Simulation of Jack-Up Dynamics With the Extremes of a Gaussian Process," *Proceedings, 14th OMAE,* Copenhagen, Denmark, Vol. 1A, pp. 313–319.

Tromans, P. S., Anaturak, A., and Hagemeijer, P., 1991, "A New Model for the Kinematics of Large Ocean Waves—Application as a Design Wave," *Proceedings, 1st Offshore and Polar Engineering Conference* (ISOPE), Golden, CO, Vol. 3, pp. 64–71.